Proposal for the J-PARC 30-GeV Proton Synchrotron:

Test Experiment to Optimize $\bar{d}$ Beam Intensity at the K1.8 Beam Line of the J-PARC Hadron Experimental Facility

T. Akaishi[2], C. Curceanu[14], K. Ebata[16], Z. Feng[17], M. Fujita[5], C. Han[7], T. K. Harada[16], T. Hashimoto[1], S. H. Hayakawa[3], Y. Hong[3], Y. Ichikawa[3], T. Isobe[1], K. Itahashi[1], M. Iwasaki[1], S. Kanda[6], R. Kurata[3], D.X. Lin[7], Y. Ma[1*], R. Murayama[1], M. Niiyama[11], H. Noumi[2], H. Ohnishi[4], S. Okada[13], F. Oura[3], F. Sakuma[1], M. Sasano[1], B. Scavino[9], A. Scordo[14], R. Sekiya[16], C. Seong[3], K. Shirotori[2], F. Sirghi[14], D. Suzuki[1], K. Suzuki[2], X. Sun[7], T. Takahashi[6], T. N. Takahashi[2], U. Tamponi[8], M. Tanaka[12], K. Tanida[5], K. Tsukada[15], M. Ukai[6*], H. Wang[7], T. Yamaga[6], T. O. Yamamoto[5], X. Yuan[7], Y. Zhang[7], H. Zhang[10]

[1]RIKEN, Wako, 351-0198, Japan
[2]Research Center for Nuclear Physics, Osaka University, Osaka, 560-0043, Japan
[3]Department of Physics, Tohoku University, Miyagi, 980-8578, Japan
[4]Research Center for Accelerator and Radioisotope Science, Tohoku University, Miyagi, 982-0826, Japan
[5]Japan Atomic Energy Agency, Tokai, 319-1195, Japan
[6]KEK, Tsukuba, 305-0801, Japan
[7]Institute of Modern Physics, Chinese Academy of Sciences, Lanzhou, 730000, China
[8]INFN Sezione di Torino, Turin, Italy
[9]Department of Physics and Astronomy, Uppsala University, Sweden
[10]School of Nuclear Science and Technology, Lanzhou University, Lanzhou, 730000, China
[11]Department of Physics, Kyoto Sangyo University, Kyoto, 603-8555, Japan
[12]Faculty of Science and Engineering, Waseda University, Tokyo, 169-8555, Japan
[13]College of Science and Engineering, Chubu University, Kasugai, 487-8501, Japan
[14]Laboratori Nazionali di Frascati dell' INFN, I-00044 Frascati, Italy
[15]Institute for Chemical Research, Kyoto University, Kyoto, 611-0011, Japan
[16]Department of Physics, Kyoto University, Kyoto, 611-0011, Japan
[17]School of Physics and Optoelectronics, South China University of Technology, Guangzhou 510640, China

* *Corresponding Spokespersons: Y. Ma and M. Ukai*

Executive Summary

Recently, M. Ukai *et al*. confirmed the existence of antideuteron ($\bar{d}$) as secondary beam at J-PARC K1.8 beam line [1]. This discovery provides a unique opportunity to study antimatter composed of multiple antinucleons. However, due to the limited data available, the $\bar{d}$ beam intensity and the optimal beam line setup remain unknown.

In this proposal, we aim to establish the optimal beam line configuration for $\bar{d}$ beam at the K1.8 beam line of the J-PARC Hadron Experimental Facility(HEF). This will establish a solid foundation for future $\bar{d}$ beam experiments, such as the $\bar{d}$+^{12}C reaction experiment proposed by us in July 2024 [2].

The major parameters of this experiment are summarized below:

Beam line	:	K1.8
Apparatus	:	K1.8 beam line
Purpose I	:	Optimize $\bar{d}$ yield for 1.8 GeV/c beam momentum
Beam time	:	87 Tppp $\times$ 8 hours (87×10^{12} proton per pulse corresponds to 80 kW beam power on Au production target.)
Purpose II	:	Search for $\bar{d}$ for lower momentum ($<$ 1.8 GeV/c)
Beam time	:	87 Tppp $\times$ 16 hours

Contents

1 Introduction

Antimatter has held a significant position within both the scientific community and popular culture for many years. It has captured attention ranging from testing CPT violation [3, 4] to its portrayal in Hollywood movies [5], symbolizing humanity's unrelenting pursuit of the unknown. The investigation into antimatter and its dynamic interplay with matter remains intricately intertwined with one of contemporary physics' most profound enigmas: the antimatter-matter imbalance. Numerous investigations into antiprotons ($\bar{p}$) and their interaction with matter have been undertaken to address this puzzle [6].

However, the exploration of antinuclei composed of multiple antinucleons, such as the antideuteron ($\bar{d}$), remains relatively unexplored territory. For instance, only absorption cross sections on heavy targets are reported at 13.3 GeV/c and 25 GeV/c without information about their reaction products as shown in Fig. 1 [7, 8]. A recent study by the ALICE collaboration shown in Fig. 2 provides the total inelastic cross section between $\bar{d}$ and the averaged detector materials ($< A >= 17.4$ and $< A >= 31.8$) as effective targets, without details about the reactions [9].

In this proposal, we will first describe our motivation to study the $\bar{d}$ related physics and summarize the current situation for the $\bar{d}$ beam availability. After that, we will present results for $\bar{d}$ beam at J-PARC HEF K1.8 and K1.8BR beam line as a basis for the current proposal. Finally, we will outline a plan for optimizing the $\bar{d}$ beam and request beam time for this test experiment proposal.

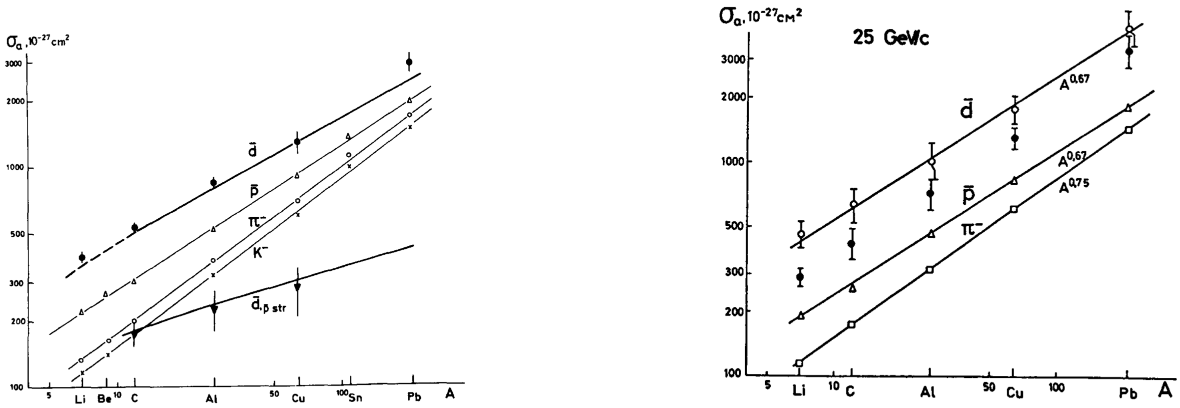

(a) $\bar{d}$ absorption cross section with various targets at 13.3 GeV/c [7].

(b) $\bar{d}$ absorption cross section with various targets at 25 GeV/c [8].

Figure 1: $\bar{d}$ absorption cross section measured in 1970s at JINR.

1.1 Physics Motivation for Utilizing $\bar{d}$ Beam

In a previously submitted LOI, we propose to investigate the antideuteron using a $\bar{d}$ beam at the K1.8 beam line of the J-PARC Hadron Experimental Facility [2]. Specifically, we aim to address the following topics:

1. How does $\bar{d}$ interact with nucleus? By adding one more antinucleon, how will the $\bar{d}-$nucleus potential differ from $\bar{p}-$nucleus?

2. How will the antinucleus annihilate with nucleus? Will the two antinucleons inside $\bar{d}$ annihilate with nucleons from nucleus independently or simultaneously?

1.1.1 Study $\bar{d}-$nucleus Optical Potential

The interaction between antimatter and matter has been a topic of fundamental importance since the discovery of the antiproton in 1955 [10]. Within the framework of Relativistic Mean Field Theory (RMF), the $\bar{p}-$nucleus interaction is expected to be extraordinarily strong due to the flip of G-parity.

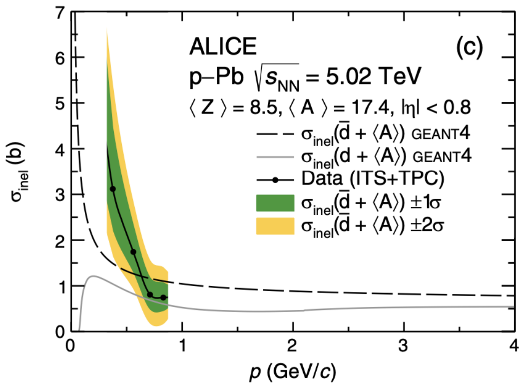

(a) $\bar{d}$ inelastic cross section with P $<$ 1.0 GeV/c.

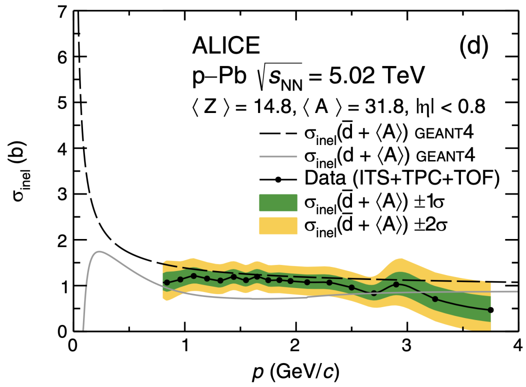

(b) $\bar{d}$ inelastic cross section with P $>$ 1.0 GeV/c.

Figure 2: Inelastic cross section of $\bar{d}$ on ALICE detector as effective target [9].

This flip results in both the scalar and vector potentials becoming attractive, a situation that is usually canceled out in the case of nucleons. A calculation performed exploiting the G-parity flipping returns a potential of of $V \sim -600$ MeV [11].

However, experimental results from both $\bar{p}$-atomic X-ray measurements [12, 13] and $\bar{p}-$nucleus elastic scattering experiments [14] suggest a much weaker interaction, with $V \sim -100$ MeV. One possible explanation for this discrepancy is the large probe distance in both approaches, which makes them sensitive only to the long-range part of the potential. In contrast, the $\bar{p}$ absorption cross section is expected to be more sensitive to the short-range part by penetrating into the nuclear medium and causing absorption. For instance, $\bar{p}$ at 0.6 GeV/c can reach an average of 50% nuclear density before absorption occurs. In this case, the potential is derived as $V \sim -150$ MeV [11].

Another important factor contributing to the deviation from the RMF prediction is the short lifetime of the $\bar{p}-$nucleus system. Regardless of the experimental approach mentioned above, the virtual potential obtained so far consistently shows $W \geq 100$ MeV. Such a strong virtual potential (i.e. the short lifetime) makes it difficult for the $\bar{p}$ nucleus state to reach an equilibrium state before annihilation, which is required by the RMF prediction.

While we have some understanding of the $\bar{p}-$nucleus interaction, the $\bar{d}-$n interaction remains an open question. The $\bar{d}$ nucleus is composed of two antinucleons, making it a unique system for studying multiple $\bar{N} - N$ interactions. If we assume the $\bar{d}-$nucleus system has a similar lifetime to that of the $\bar{p}-$nucleus system, a linear extrapolation from the $\bar{p}-$nucleus potential gives $V - 200 \sim -300$ MeV due to the presence of two attractive centers. This raises the question: Will such a strong attractive potential modify the nucleus structure and the lifetime of the $\bar{d}-$nucleus system? This is one of the key questions we aim to address in this proposal.

In order to investigate quantitatively the $\bar{d}-$nucleus interaction, we will utilize GiBUU, a transport model-based calculation package developed by Giessen University, Germany [15]. GiBUU has been widely used to study $\bar{p}-$nucleus interactions, showing impressive agreement with experimental data [11]. Thanks to the kind support of Dr. K. Gallmeister of the GiBUU group, a $\bar{d}$ beam is now available in the GiBUU package.

To motivate and support our proposal, we performed calculations for the $\bar{d}+^{12}$C reaction with different strengths for the real part of the optical potential. We found that the ratio between partial (σ_{ParAnn}) and coherent (σ_{CohAnn}) annihilation cross sections is very sensitive to the strength of the optical potential. Here, partial annihilation refers to the reaction where only one antinucleon from $\bar{d}$ annihilates with a target nucleon, while coherent annihilation refers to the reaction where both antinucleons from $\bar{d}$ annihilate with target nucleons.

More specifically, for a $\bar{d}$ beam at 1.8 GeV/c, if we assume $V = -150$ MeV between $\bar{N}-$nucleus as derived from $\bar{p}-$nucleus absorption experiment data, the ratio $\sigma_{ParAnn}/\sigma_{CohAnn}$ is approximately 2.8.

If we set $V = -300$ MeV between $\bar{N}-$nucleus, the ratio $\sigma_{ParAnn}/\sigma_{CohAnn}$ becomes 1.6, indicating a sensitive dependence. This observation suggests that the ratio between these two cross sections can be used to derive the strength the $\bar{d}-$nucleus optical potential.

From an intuitive perspective, the sensitivity of the ratio $\sigma_{ParAnn}/\sigma_{CohAnn}$ regarding the $\bar{d}-$nucleus optical potential becomes apparent when considering the attractive force between the $\bar{d}$ and the nucleus. A stronger force draws the antinucleons nearer to the nucleus, consequently increasing the likelihood of coherent annihilation. [1]

1.1.2 Investigate Multiple $\bar{N}-N$ Annihilation Mechanism

Another interesting topic will be addressed in this experiment is the multiple $\bar{N}-N$ annihilation mechanism. In order to facilitate the discussion, we classify the $\bar{d}$+^{12}C coherent annihilation into the following three scenarios:

1. Two-Step Independent Annihilation: This involves two independent $\bar{N}-N$ pairs, each annihilating without affecting the other, akin to having two separate $\bar{p}-p$ annihilation.
2. Correlated Cascade Annihilation: In this scenario, one of the mesons produced from the first $\bar{N}-N$ annihilation is absorbed by the second pair before their reaction. The sequence of reactions is: $\bar{N}+N \to (n-1)\pi$, $\pi+\bar{N} \to \bar{\Delta}$ (or $\pi+N \to \Delta$), and $\bar{\Delta}+N \to n\pi$ (or $\Delta+\bar{N} \to n\pi$). Consequently, the second annihilating pair will have a larger phase space available for annihilation reaction due to the increase in total energy.
3. One-Step Simultaneous Annihilation: If both $\bar{d}$ and ^{12}C are in a short-range correlated (SRC) state during $\bar{d}-2N$ annihilation, the annihilation phase space can expand up to 4.5 GeV. This extreme case will produce pions with high momentum beyond the kinematic limits of the other two scenarios.

At first glance, all three scenarios produce high-multiplicity final states, making it challenging to distinguish them experimentally. However, the well studied $\bar{p}-p$ annihilation can provide valuable insights. As shown in Figs. 3 and 4, multiple $\pi^{\pm,0}$ final states dominate $\bar{p}-p$ annihilation at rest [**?**]. A Gaussian fit to the multiplicity distribution in Fig. 3 yields a mean multiplicity of 5.01 and a standard deviation of $\sigma = 1.04$. The $\pi^{\pm,0}$ momentum distribution in Fig. 4 closely resembles a pure phase space distribution, suggesting that $\bar{p}-p$ annihilation can be understood as a reconfiguration of $\bar{q}-q$ pairs with equal probability.

This observation suggests that the π momentum distribution can be exploit to distinguish experimentally between the three annihilation scenarios in the $\bar{d}$+^{12}C system. Specifically, the total phase space is dictated by the initial total energy, and the multiplicity is directly proportional to the energy available for the annihilation reaction. Drawing from the insights gained from $\bar{p}-p$ annihilation studies, where the multiplicity of the final state $\pi^{\pm,0}$s is crucial, we hypothesize that the π multiplicity correlates with the total energy of the annihilation partners.

For the One-step Simultaneous Annihilation, we propose the following relations:

$$\begin{aligned} \text{multiplicity} &= \frac{\text{total energy of } \bar{d}+2N}{\text{mass of } \bar{p}+p} \times 5.01 \\ \sigma &= \frac{\text{total energy of } \bar{d}+2N}{\text{mass of } \bar{p}+p} \times 1.04, \end{aligned} \tag{1}$$

where 5.01 and 1.04 are the mean and standard deviation of π multiplicity from $\bar{p}-p$ annihilation at rest, respectively. Similarly, for a correlated cascade annihilation, we can determine the total energy of the $\bar{\Delta}+N$ (or $\Delta+\bar{N}$) system by combining a random pion from the first annihilation with the second $\bar{N}-N$ pair. The resulting π momentum distribution is depicted in Fig. 5, 6, and 7.

[1] One should note that if the so obtained potential between $\bar{d}$ and nucleus is not so extraordinarily strong that the distortion for the $\bar{d}$ and nucleus wave function are negligible, the $\bar{d}$+^{12}C coherent annihilation cross section can be used to derive the $\bar{d}$ radius for the first time, which is a key to allow us to test the nuclear force universality.

The branching ratio for Correlated Cascade Annihilation is estimated to be 1/3 of all coherent annihilation events, based on normalization with GiBUU-calculated coherent events for $P \geq 1.6$ GeV/c. Consequently, the branching ratio for Two-Step Independent Annihilation is estimated at 2/3. Finally, the branching ratio for One-Step Simultaneous Annihilation is estimated at 4% of all coherent annihilation events, taking into account that the SRC state in $\bar{d}$ and ^{12}C occurs with a probability of 20% each.

For the two-step independent annihilation, characterized by a phase space of approximately 2.24 GeV for a $\bar{p}$ beam at 0.9 GeV/c, the π momentum distribution extends up to ~ 1.6 GeV/c. In contrast, the one-step simultaneous annihilation yields a phase space roughly twice as large as the independent case, amounting to approximately 4.5 GeV. Consequently, the resulting π momentum distribution exhibits a much broader spread, extending beyond the kinematic limit observed in the $\bar{p} - p$ case. In the case of correlated cascade annihilation, the π momentum distribution falls between the ranges observed in these two extreme scenarios. [2]

To further validate the proposed method, we calculated the $\bar{d}$+^{12}C reaction using the GiBUU package with default parameters optimized for the $\bar{p}$ data. The calculated π momentum distribution for partial and coherent annihilation from $\bar{d}$+^{12}C reaction is shown in Fig. 8 and 9, respectively. The slight excess of π momentum than 1.6 GeV/c in partial annihilation visible in Fig. 8 is due to the Fermi motion contribution, which is about $\sim 10\%$ of the signal events given in Fig. 9. Fig. 9 shows the highest number of events above the kinematic limit as a result of the Correlated Cascade Annihilation from GiBUU. [3] The results are consistent with our phase space based estimation, indicating that the π momentum distribution can be used to distinguish between the three annihilation scenarios.

Before concluding this section, we would like to point out that the proposed measurement for the One-Step Simultaneous Annihilation provides a unique opportunity to study the short-range correlated (SRC) state in both $\bar{d}$ and ^{12}C nucleus in spatial distribution. The SRC state is an important topic which might be related to the EMC effect. However, the study of the SRC so far has been limited to the momentum space: what has been observed in the electron scattering data is the back-to-back correlation of high-momentum nucleons [16]. One has to rely on the uncertainty principle to infer the spatial distribution from the momentum distribution. In our proposed experiment, the One-Step Simultaneous Annihilation, if observed, can only come from very tight spatial overlap of the $\bar{d}$+^{12}C wave functions. Therefore, we will have the first chance to verify the SRC state in spatial distribution.

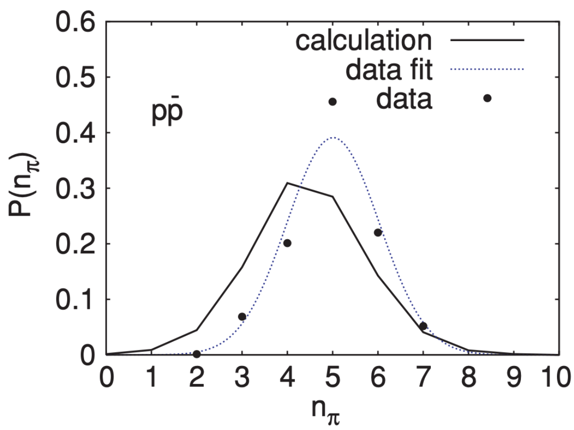

Figure 3: π multiplicity from $\bar{p}-p$ annihilation at rest.

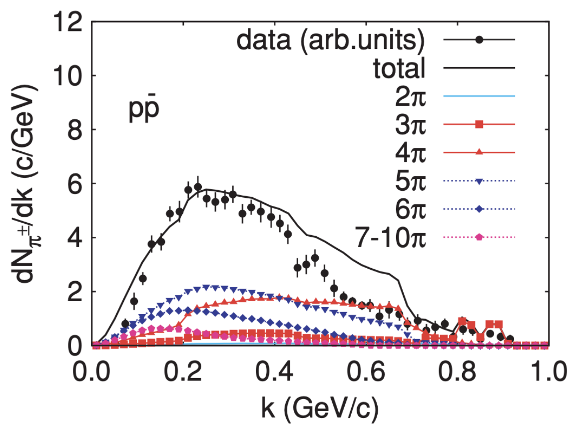

Figure 4: π momentum distribution from $\bar{p} - p$ annihilation at rest.

[2]Qualitatively, the rationale for utilizing the π momentum distribution to distinguish between the three scenarios is as follows: the kinematic constraints governing the π momentum distribution are directly linked to the annihilation phase space, which scales with the total energy of the annihilation partners.

[3]One should note that, however, the One-Step Simultaneous Annihilation is not included in the GiBUU calculation.

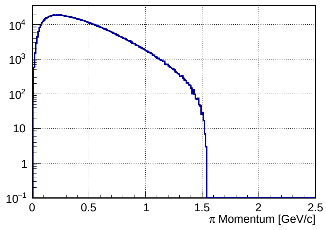

Figure 5: $\pi^{\pm}$ momentum distribution from Two-Step Independent Annihilation with 10^6 $\bar{d}$ beam particles on ^{12}C target.

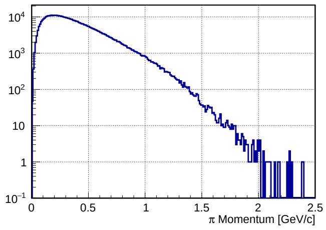

Figure 6: $\pi^{\pm}$ momentum distribution from Correlated Cascade Annihilation with 10^6 $\bar{d}$ beam particles on ^{12}C target.

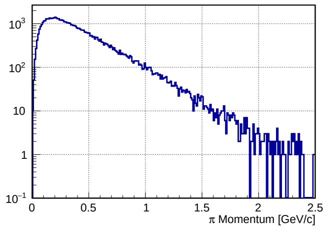

Figure 7: $\pi^{\pm}$ momentum distribution from One-Step Simultaneous Annihilation with 10^6 $\bar{d}$ beam particles on ^{12}C target.

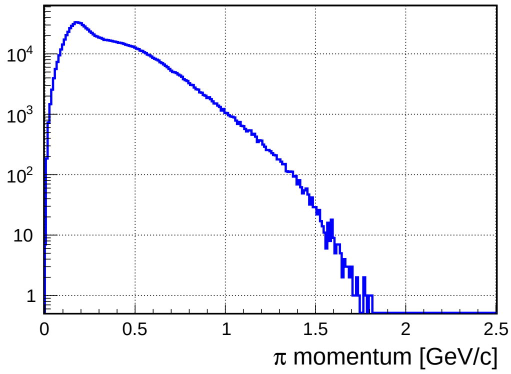

Figure 8: π momentum distribution from $\bar{d}$+^{12}C partial annihilation events.

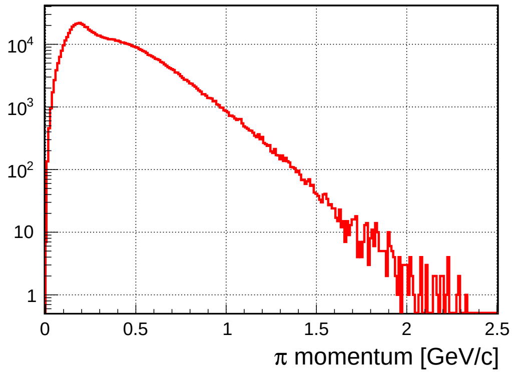

Figure 9: π momentum distribution from $\bar{d}$+^{12}C coherent annihilation events.

1.2 Overview for the $\bar{d}$ beam status

Due to the low production rate and high production threshold, the $\bar{d}$ beam has not been widely available. Before Ukai's recent report [1], the only available data comes from the JINR Dubna in 1970s [17], which enables the absorption cross section measurement for $\bar{d}$ with various targets [7, 8]. In this section, we will summarize the results from JINR and current situation J-PARC HEF [1].

1.2.1 Previous $\bar{d}$ production study at JINR

In 1970s, there were a series of experiments conducted at JINR to study the $\bar{d}$ production and absorption cross section. The $\bar{d}$ production cross section was measured in p+Be, p+Al collision at 70 GeV proton beam energy [17]. The $\bar{d}$ absorption cross section was measured with various target at both 13.3 GeV/c and 25 GeV/c $\bar{d}$ beam momentum as shown in Fig. 1a and Fig. 1b.

The results for $\bar{d}$ production are summarized in Fig. 10 and Fig. 11. Some characteristic features are: 1) both $\bar{p}$ and $\bar{d}$ production cross sections are maximized around 13 GeV/c momentum; 2) the $\bar{d}/\bar{p}$ yield ratio is also peaked at 13 GeV/c. These behaviors can be understood by employing the coalescence model, in which the formation of $\bar{d}$ is described by the combination of two antinucleons that aligned with small relative momentum. Based on this interpretation, the $\bar{d}$ yield is proportional to the product of $\bar{p}$ and $\bar{n}$ yield, which is maximized when both $\bar{p}$ and $\bar{n}$ have highest yield.

Another important parameter from JINR results is the yield ratio between $\bar{d}$ and $\bar{p}$, which gives $\bar{d}/\bar{p} \sim 10^{-4}$ as shown in Fig. 10. If we rely on the coalescence model, this ratio is sensitive to the primary proton beam energy because of the multiple-antinucleon production cross section. As will be introduced, for J-PARC HEF K1.8 beam line, this ratio is in the order of 10^{-6}, which is much lower than the JINR results. This difference can be attributed to the lower primary proton beam energy at J-PARC as 30 GeV compared to 70 GeV at JINR as the lower primary proton beam energy results in a lower double antinucleon production cross section, which in turn leads to a lower $\bar{d}/\bar{p}$ yield ratio.

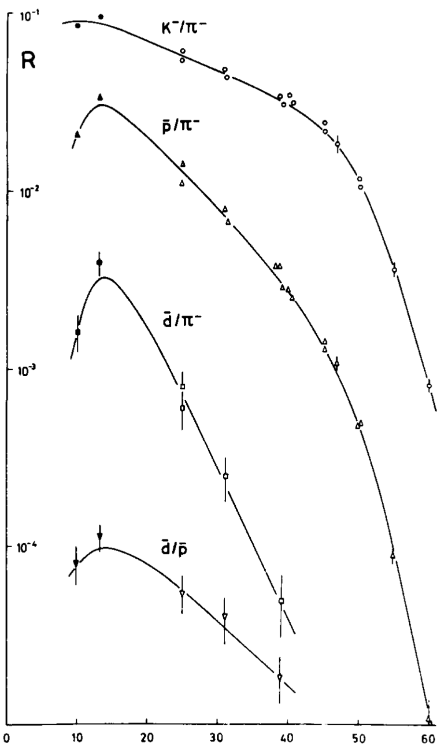

Figure 10: K^-/π^-, $\bar{p}/\pi^-$, $\bar{d}/\pi^-$ and $\bar{d}/\bar{p}$ yield ratio from p+Al/Be target collision at 70 GeV [17].

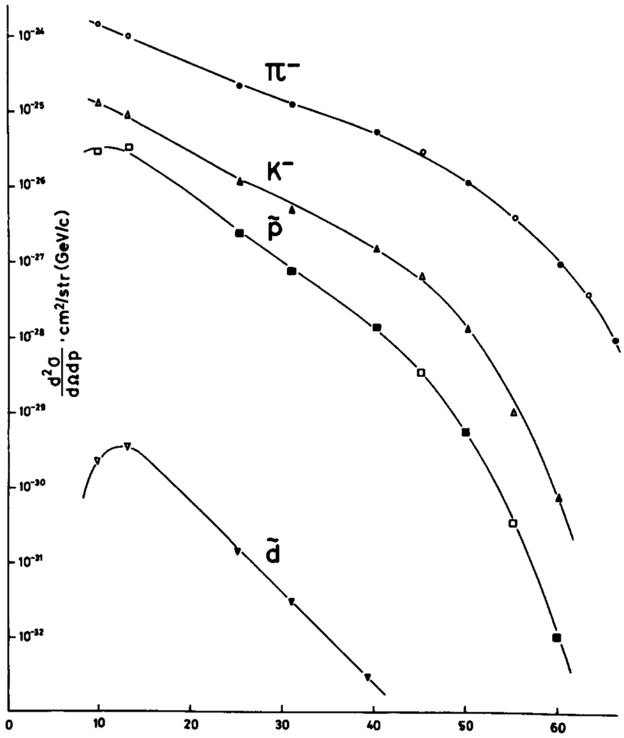

Figure 11: Differential cross section for $\pi^-/K^-/\bar{p}/\bar{d}$ production in $p-$Al collision at 70 GeV [17].

1.2.2 Current $\bar{d}$ beam status at J-PARC HEF

There are two studies to identify the $\bar{d}$ beam at both J-PARC HEF K1.8 and K1.8BR beam lines. The schematic layout of these two beam lines is shown in Fig. 12. The main difference between these two beam lines is the momentum rage: K1.8 beam line is optimized for 1.8 GeV/c beam momentum while K1.8BR beam line is optimized for lower momentum ($\sim$ 1.0 GeV/c) beam. The first stage Electro Static Separator (ESS) is common for both beam lines but the second stage ESS is only available for K1.8 beam line.

In a preliminary study conducted by one of the authors, M. Ukai, the presence of a $\bar{d}$ beam at a momentum of 1.8 GeV/c was confirmed, with a yield of approximately 0.3 $\bar{d}$ particles per spill (where 1 spill lasts about 5 seconds) at a beam power of 70 Tppp using the J-PARC HEF K1.8 beam line [1]. The $\bar{d}/\bar{p}$ production ratio was estimated to be around 10^{-6}. However, due to the limited duration of this initial study (approximately 3 hours), the K1.8 beam line was not fully optimized for $\bar{d}$ beam transportation. Optimizing the beam line for enhanced $\bar{d}$ yield is a key motivation for the current proposal.

Another trial to identify the $\bar{d}$ beam at 1.0 GeV/c was conducted at J-PARC HEF K1.8BR beam line in 2023 [18]. In this study, only one $\bar{d}$ candidate was identified using energy deposit and TOF information corresponding a yield of 1 $\bar{d}$/2 hours at 54 Tppp beam power. For details of the study, please refer to Sec. 2.2.

The drastic drop in the $\bar{d}$ yield at 1.0 GeV/c compared to the previous study at 1.8 GeV/c can be explained by considering the $\bar{p}$ yield. According to Ref. [19], the $\bar{p}$ yield from 20 GeV primary proton beam is maximized at 3.0 GeV/c and drastically drops for lower momentum. This behavior can be used to understand the momentum dependence of the $\bar{d}$ beam yield. Consequently, the $\bar{d}$ beam yield at J-PARC HEL is supposed to be maximized at ~7.0 GeV/c, which will be a topic to be addressed in the future.

Table 1 summarizes the results of the $\bar{d}$ beam study at J-PARC HEF K1.8 and K1.8BR beam line.

Table 1: J-PARC HEF K1.8 and K1.8BR beam line results summary

Beam line	Momentum (GeV/c)	MR intensity /spill	$\bar{d}$/spill	$\bar{p}$/spill	$\bar{d}/\bar{p}$ ratio	Slit opening IFV/MS1/MS2	Date
K1.8	1.8	70T	~ 0.30	300k	$\sim 10^{-6}$	2.2/5.0/5.0	June 2021
K1.8	1.8	72T	~ 0.34	1.5M	$\sim 0.2 \times 10^{-6}$	2.2/5.0/5.0	May 2024
K1.8BR	1.0	54T	$< 10^{-3}$	200k	$< 10^{-9}$	4.0/4.7/N.A.	June 2023

1.2.3 Impact for $\bar{d}$ beam at J-PARC HEF

The confirmation of a $\bar{d}$ beam at J-PARC HEF K1.8 beam line will open up a new avenue for studying the antinucleus with multiple antinucleons. In particular, we have proposed to study the $\bar{d}$−nucleus interaction and the multiple $\bar{N} - N$ annihilation mechanism [2]. In addition, the $\bar{d}$ yield itself from p+Au collision is an interesting topic, which can help us to understand the $\bar{d}$ production mechanism and high energy hadronization process.

In this proposal, we aims to optimize the 1.8 GeV/c $\bar{d}$ beam condition at the K1.8 beam line as it will directly affect the beam time request and statistics for our LOI [2]. In addition, as will be described later, we will also explore the momentum dependence of the $\bar{d}$ beam yield to understand the $\bar{d}$ production mechanism.

2 Previous $\bar{d}$ beam studies at J-PARC HEF

2.1 Specifications of K1.8 and K1.8BR beam line

The K1.8 and K1.8BR beam lines are secondary beam lines designed to deliver mass-separated secondary particles produced at the primary target (T1) using the high-intensity proton beam from the MR. Figure 12 illustrates the schematic layout of the K1.8 and K1.8BR beam lines, with their specifications summarized in Table 2. Both beam lines share a common structure comprising two main sections: the extraction section from the T1 target to the intermediate focus (IF) point and the first electrostatic mass separator (IF - MS1).

The K1.8BR beam line includes an additional section for beam momentum analyzer, while the K1.8 beam line features two additional sections: the second electrostatic mass separator (D3-MS2) and its own beam momentum analyzer. At the intermediate focus point, the beam is vertically focused, allowing the vertical slit (IFV) to eliminate unwanted particles, such as cloud pions from K_S^0 decays.

Each electrostatic separator (ESS) is positioned between correction magnets (CMs). The ESS has a length of 6 m with a 10 cm gap. The CMs are vertical bending dipole magnets that provide beam trajectory correction. Furthermore, mass slits (MS) are positioned downstream of the corresponding CMs. These systems work together to provide a high-purity kaon beam for each beam line.

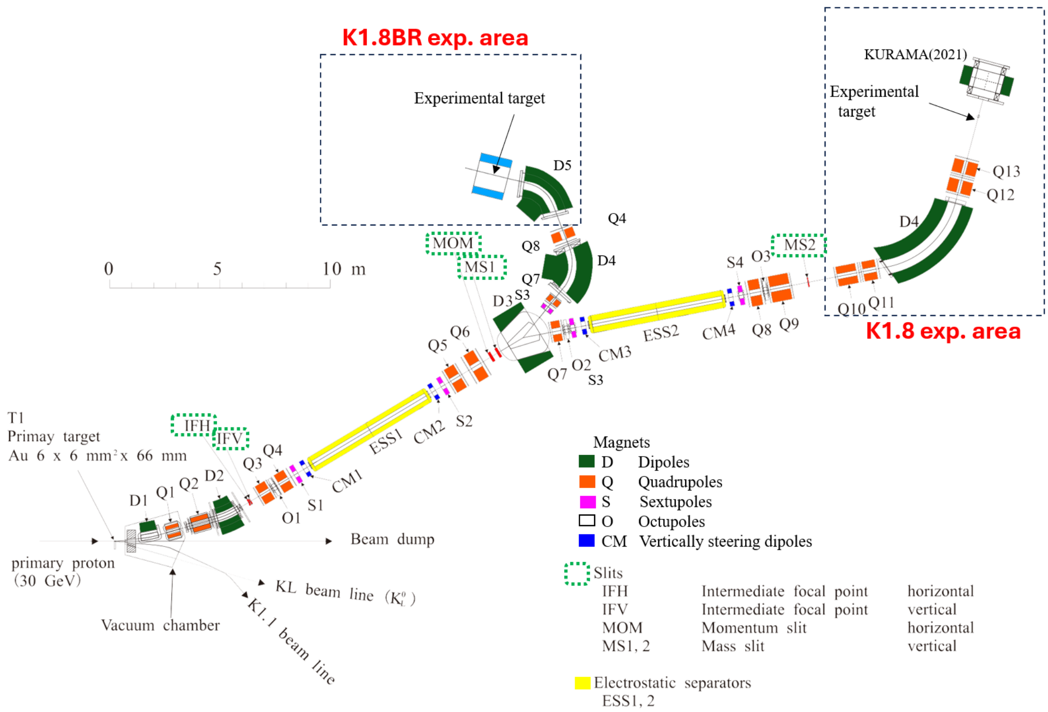

Figure 12: Schematic view of the J-PARC HEF K1.8 and K1.8BR beam lines.

2.2 Results of the $\bar{d}$ beam study for 1.0 GeV/c at K1.8BR beam line

A test experiment, T98, was conducted at the K1.8BR beam line in 2023 to search for the $\bar{d}$ beam at 1.0 GeV/c as a feasibility study to test liquid Argon TPC designed for dark matter search via $\bar{d}$ detection [18]. The schematic layout of the K1.8BR beam line is shown in Fig. 13. $\bar{d}$ beam particles were identified using three plastic scintillation counters in the offline analysis: BHT, T0, and DEF. The BHT is installed upstream of S3; the T0 is located downstream of D5 and the DEF is positioned before the final focus (FF).

Table 2: Specification of the K1.8 and K1.8BR beam lines

Primary target (T1)	Au 66-mm thickness
Extraction angle	6 deg.
Momentum bite	±3%
Maximum momentum	1.8 GeV/c(K1.8), 1.0 GeV/c(K1.8BR)
Beam line length	46 m (K1.8),

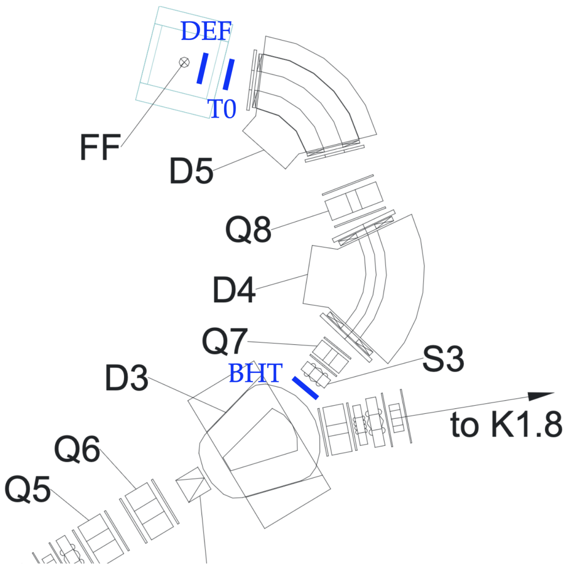

Figure 13: Schematic view of the K1.8BR experimental area.

To select $\bar{d}$ beam particle, energy deposit in the DEF and DEF-T0 TOF information were used as shown in Fig. 14. The upper panel shows the event selection based on d beam events, which are intentionally injected to the beam line to calibrate the detector and optimize the $\bar{d}$ beam condition because of the same mass of d and $\bar{d}$. The lower panel shows the event selection region from $\bar{d}$ beam runs. After the event selection, the $\bar{d}$ beam particles were identified by the Time-over-Threshold (TOT) information from the BHT and BHT-T0 TOF information as given in 15, where the $\bar{d}$ signal region is again identified by the d beam events.

As a result, only one $\bar{d}$ candidate was identified using energy deposit and TOF information corresponding a yield of 1 $\bar{d}$/2 hours at 54 Tppp beam power. The $\bar{d}$ yield at 1.0 GeV/c is much lower than the previous study at 1.8 GeV/c at K1.8 beam line. This behavior can be understood by considering the $\bar{p}$ yield and coalescence model as previously discussed.

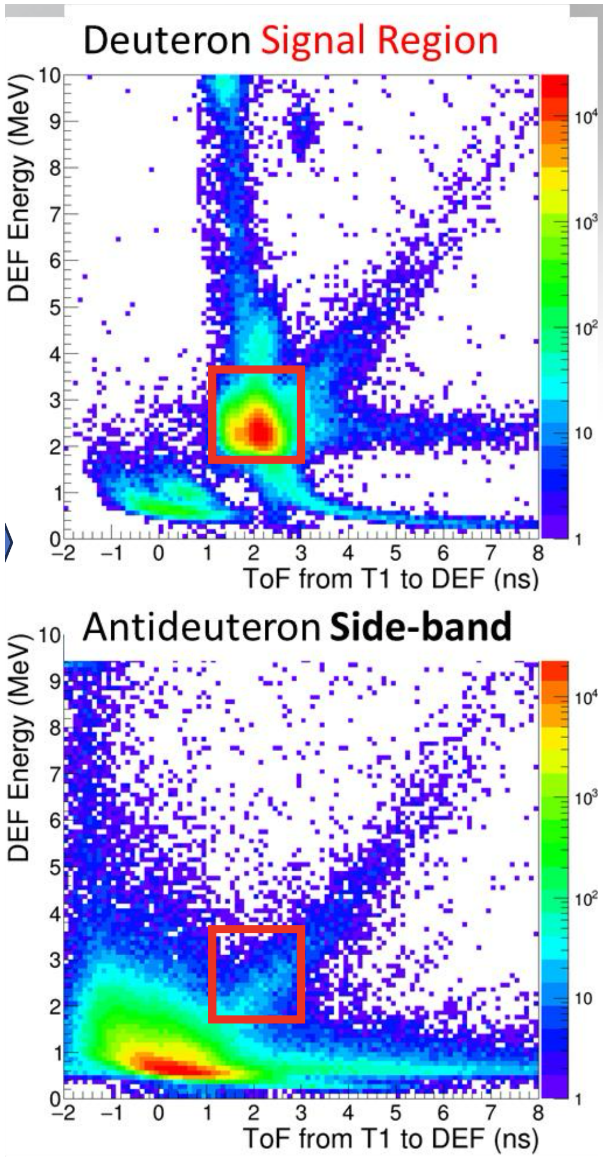

Figure 14: $\bar{d}$ event selection based on DEF-T0 information: upper panel shows the event selection based on d beam events, lower panel shows the event selection region from $\bar{d}$ beam runs. Figure is taken from M. Tanaka's presentation for J-PARC T98 test experiment.

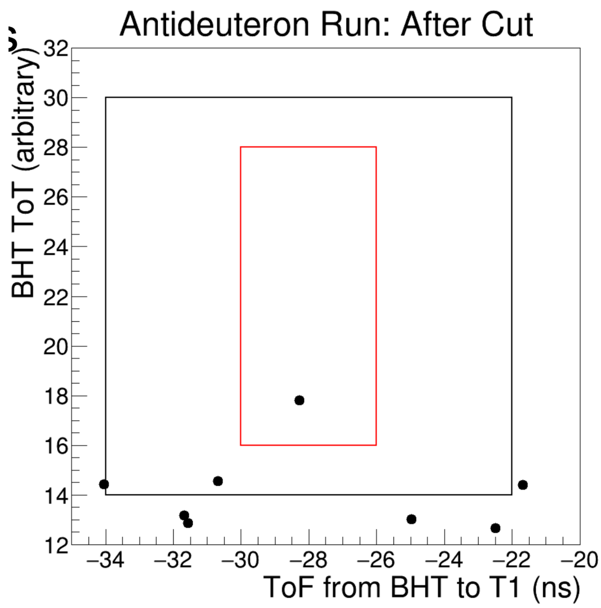

Figure 15: Result for the $\bar{d}$ search at 1.0 GeV/c at K1.8BR beam line. Only one $\bar{d}$ candidate was identified over 2 hour of beam time at 54 Tppp. Figure is taken from M. Tanaka's presentation for J-PARC T98 test experiment.

2.3 Results of the $\bar{d}$ beam study for 1.8 GeV/c at K1.8 beam line

The extraction of the $\bar{d}$ beam to the K1.8 beam line was attempted twice, in 2021 (K18'21) and 2024 (K18'24). During these attempts, an $\bar{d}$ beam intensity of approximately 0.3 counts per spill was achieved with a primary proton intensity of $\sim 70 \times 10^{12}$ protons per spill (70Tppp), as summarized in Table 3. This corresponds to a beam intensity of approximately 250 counts per hour under the current MR repetition rate of 4.24 seconds.

Notably, the K18'21 experiment marked the first successful extraction of an $\bar{d}$ beam at the J-PARC Hadron Experimental Facility (HEF). However, due to the limited test time, the beam line conditions, including the ESS settings and CM magnet currents, were not fully optimized for the $\bar{d}$ beam.

Table 3: Summary of the 1.8 GeV/c $\bar{d}$ and $\bar{p}$ beam intensities measured at the K1.8 beam line, along with their CM magnet conditions. For the $\bar{d}$ beam, the CM magnet settings were not specifically optimized but were scaled from those used for the $\bar{p}$ beam. The slit conditions, including vertical slit openings (IFV = 2.2 mm, MS1 = MS2 = 5.0 mm), are listed in Table 4.

Run	**MR intensity [proton/spill]**	**ESS1 [kV]**	**ESS2 [kV]**	**CM1/2 [A]**	**CM3/4 [A]**	$\bar{d}$ **intensity [/spill]**	$\bar{p}$ **intensity [/spill]**	**BH2 rate [/spill]**
K18'21	70T	±150	OFF	332/332	OFF	0.3		367k
				259/259	OFF		$\sim$ 300k^{*1}	
K18'24	72T	±150	±150	339/317	357/285	0.34		0.9k
				268/246	287/215		1.6M	

^{*1} p-bar intensity of K18'21 was estimated value from the measured value for MS1=MS2=1.4 mm.

The beam momentum of 1.8 GeV/c is well-studied and serves as the standard momentum at the K1.8 beam line. These tests were conducted as part of beam line studies for the 1.8 GeV/c K^- beam tuning or during MR study periods.

The slit conditions are summarized in Table 4. The IFV slit was set to an opening of 2.2 mm. Although this value is significantly smaller than the vertical profile of the primary proton beam at the T1 target ($\sigma < 2$ mm), as shown in Table 5, it was chosen to match the settings used in running physics programs (E42 in 2021 and E70 in 2024). This ensured sufficient K^- beam purity for 1.8 GeV/c operations. The MS1 and MS2 slits were set to 5 mm openings, as the beam rate was nearly saturated at this width with an IFV opening of 2.2 mm. The horizontal slits (IFH and MOM) were fully open during these tests.

Table 4: Slit opening widths for both K18'21 and K18'24 runs.

IFV (V)	IFH (H)	MOM (H)	MS1 (V)	MS2 (V)
2.2 mm	240 mm	360 mm	5 mm	5 mm

Table 5: Typical primary beam profile at the T1 target

	Mean(X)	Mean(Y)	Sigma(X)	Sigma(Y)
K18'21	0.95 mm	−0.33 mm	2.9 mm	1.9 mm
K18'24	0.62 mm	−0.29 mm	2.6 mm	1.7 mm

2.3.1 Procedure and results of the $\overline{d}$ beam study

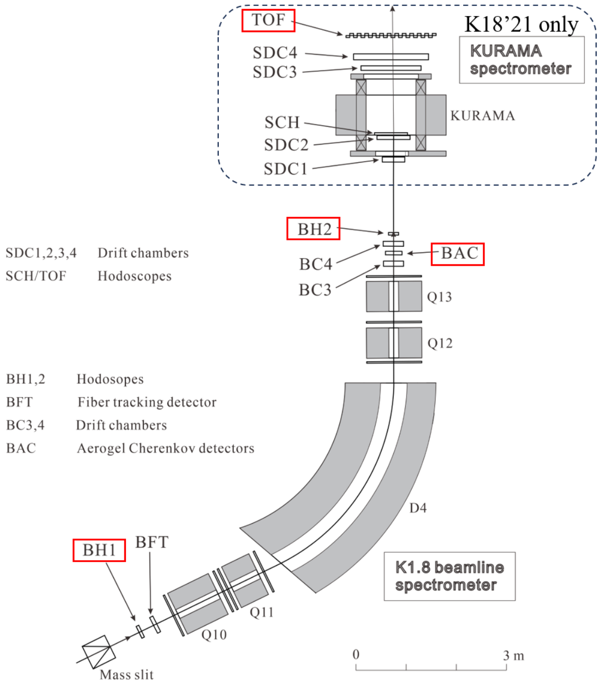

Figure 16: Schematic view and detector setup of the K1.8 beam line. The TOF detector was used only during the K18'21 run because the spectrometer for scattered particles (KURAMA) was replaced with S-2S in 2023.

Figure 16 provides a schematic view of the K1.8 experimental area. BH1, BH2, and TOF were Time-of-Flight (TOF) counters made of plastic scintillators, with flight lengths of 11.2 m for BH1-BH2 and 4.2 m for BH2-TOF. The spectrometer for scattered particles was replaced from KURAMA to S-2S between the '21 and '24 runs, resulting in the TOF counter being used only during the '21 run. Notably, the 1.8 GeV/c beam cannot traverse the S-2S spectrometer due to its limited bending power. The BAC counter, a threshold-type aerogel Cherenkov detector with a refractive index of $n = 1.03$, was employed to count the $\overline{p}$ beam rate in real-time. In this study, $\overline{d}$ particles were identified using the Time-of-Flight distribution in the offline analysis.

Initially, CM currents for the $\overline{p}$ beam were scanned online by using the counting rate of the BH2$\times\overline{\mathrm{BAC}}$ logic, as shown in Fig. 17. The CM currents for the $\overline{d}$ beam were then set by scaling the $\overline{p}$ beam currents by a factor of $\beta_{\overline{d}}/\beta_{\overline{p}}$, as CM currents are generally proportional to $1/\beta$. Although it is known from prior experience at the K1.8 beam line that the optimal CM currents often deviate from this scaled value, the currents were fixed at the scaled values due to the practical challenges of limited study time.

Figure 18 displays the Time-of-Flight distributions with CM currents configured for the $\overline{d}$ beam. Panels (a), (b), and (c) show the distributions between the BH1 and the BH2 (BH1-BH2), while (c) also includes the correlation between the BH1-BH2 and BH2-TOF. Panels (a)-(c) were taken during the K18'21 run, and panel (d) was taken during the K18'24 run. In these spectra, the timing of the π^- beam was calibrated to zero. Based on these spectra, the $\overline{d}$ beam intensities were determined, as summarized in Table 3. The corresponding $\overline{p}$ beam intensities under the same slit conditions were also measured. However, for the K18'21 run, the $\overline{p}$ beam intensity was not directly measured but was instead scaled from the measured value with MS1,2 set to a 2.8 mm opening.

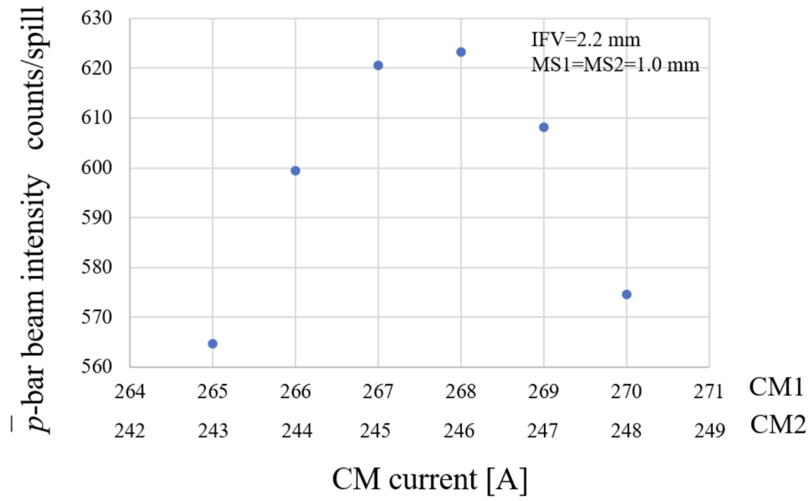

Figure 17: The intensity of the 1.8 GeV/c $\overline{p}$ beam as a function of the CM current at the K1.8 beam line, measured during the K18'24 run. The CM offset value, defined as the difference between the CM1 and CM2 currents ($\pm$11 A), was optimized to maximize the K^- beam intensity.

2.3.2 Comparison of K18'21 and K18'24 results and future outlook

At the K1.8 beam line, it is known that beam intensity is higher with the ESS turned ON than OFF. However, insufficient optimization of the CM currents can lead to significant beam intensity reduction due to the two-stage ESS. After adjustments, the $\overline{p}$ beam intensity improved drastically from approximately 300k to 1.6M counts. In contrast, the $\overline{d}$ beam intensity remained nearly unchanged. This result suggests that the $\overline{d}$ beam intensity could potentially be increased by a factor of five or more with proper optimization.

Additionally, after turning on the 2nd stage ESS in K1.8'24, an improved signal-to-noise (S/N) ratio of the $\overline{d}$ beam was observed in the BH1-BH2 TOF as shown in Fig. 18 (d). This discovery suggests that an in beam CM current scan to maximize the $\overline{d}$ beam intensity is possible by using online BH1-BH2 TOF distribution. Figure 19 shows an example of beam intensity as a function of the IFV opening width. As demonstrated, K^- beam intensity could be more than doubled with wider IFV settings. However, increasing the IFV width may degrade the S/N ratio.

As described above, a significant increase in $\overline{d}$ beam intensity is expected after optimizing CM currents and slit conditions. However, it is essential to conduct measurements to confirm these improvements while taking the S/N ratio into consideration.

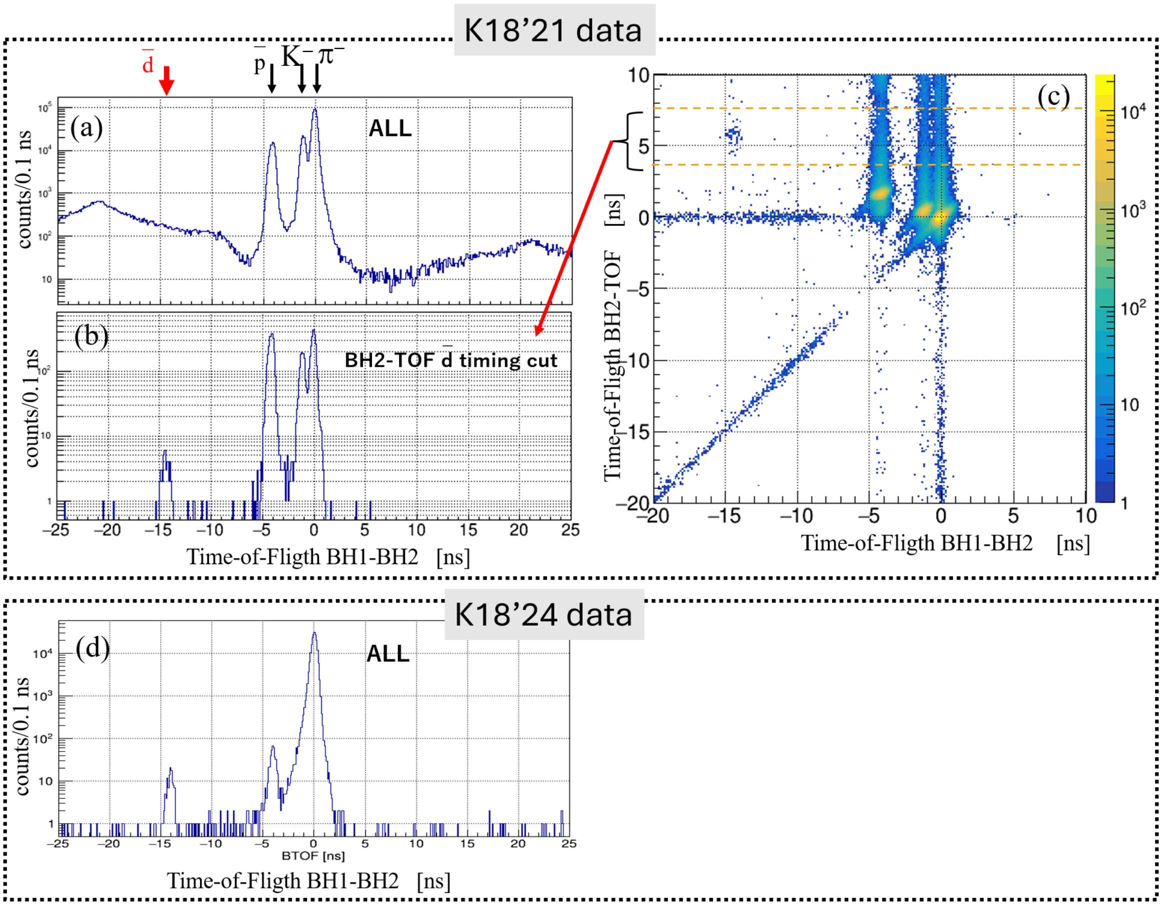

Figure 18: Time-of-Flight distributions with CM currents configured for the $\overline{d}$ beam. Panels (a), (b), and (c) show the distributions between BH1 and BH2, with panel (c) additionally showing the correlation between BH1-BH2 and BH2-TOF. Panels (a)-(c) were taken during the K18'21 run, while panel (d) was recorded during the K18'24 run. In all distributions, the timing of the π^- beam was calibrated to zero.

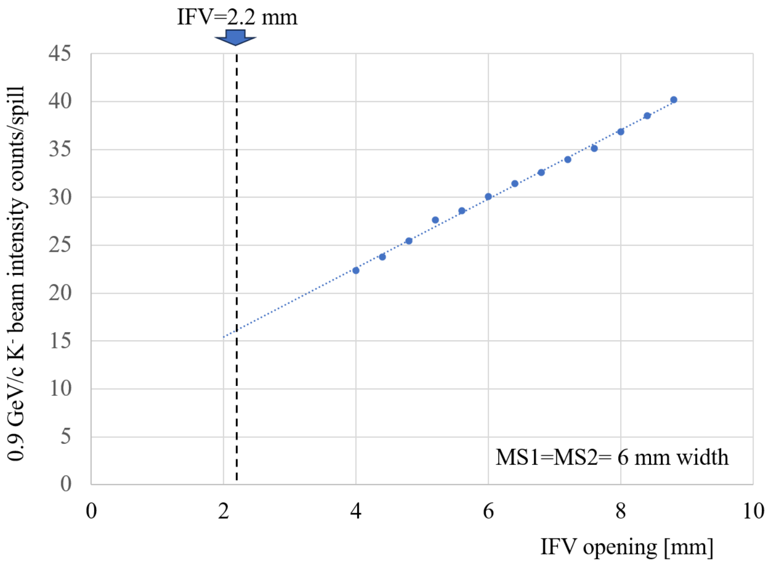

Figure 19: A sample of the beam intensity as a function of the IFV opening width, measured for the 0.9 GeV/c K^- beam at the K1.8 beam line.

3 Plan for the proposed experiment

As described in the previous sections, the $\bar{d}$ beam yield at the K1.8 beam line is ~ 0.3 $\bar{d}$/spill. This discovery is a significant step towards realizing the proposed $\bar{d}$ physics program at J-PARC. However, the $\bar{d}$ beam yield can be further optimized by tuning the beam line configurations. In this section, we will discuss the potential improvements for the $\bar{d}$ beam yield and the operation plan for the proposed experiment.

To gain a rough expectation of the $\bar{d}$ beam yield, we can scale the $\bar{d}$ yield based on the $\bar{p}$ beam intensity. Using similar beam line parameters, the $\bar{p}$ beam intensity at the K1.8 beam line is $\sim 0.3 \times 10^6$ $\bar{p}$/spill, which corresponds to a $\bar{d}/\bar{p} \sim 10^{-6}$ ratio. However, from the previous beam study, we can expect several times higher $\bar{p}$ beam intensity by optimizing the beam line configuration. If we assume the $\bar{d}$ beam yield scales with the $\bar{p}$ beam intensity, we can expect to increase the $\bar{d}$ beam yield much higher than ~ 1.0/spill.

Specifically, we will optimize the $\bar{d}$ yield and S/N by tuning the beam line parameters such as CM1/2, CM3/4, IFV/H and MS1/2. In particular, we have confirmed that by turning on the 2nd ESS a drastic improvement of the $\bar{d}$ signal to noise ratio can be achieved. This will allow us to estimate the $\bar{d}$ beam yield at the K1.8 beam line with online BH1-BH2 TOF alone.

It is also important to note that the proposed experiment will not interfere with the ongoing physics programs at J-PARC such as E70. The proposed experiment will use the same BH1, BH2, and DAQ systems that are already in place at the K1.8 beam line.

The operation plan for the proposed test beam experiment is as follows:

- **Optimization of $\bar{d}$ yield and S/N for 1.8 GeV/c beam momentum**

  A $\bar{d}$ beam at 1.8 GeV/c has been identified in our Letter of Intent (LOI) as the optimal setup to explore the $\bar{d}$-nucleus optical potential and the mechanisms underlying multiple $\bar{N}$-N annihilation [2]. Achieving the highest possible $\bar{d}$ yield at this momentum is essential, as it will directly influence the required beam time and the statistical accuracy of the experiment. To maximize the $\bar{d}$ yield, we will systematically tune the beam line parameters, including the ESS voltage and CM currents, as well as other relevant settings. We expect to complete this tuning process with 8 hours of beam time.

- **Exploration of $\bar{d}$ yield at lower beam momenta (<1.8 GeV/c)**

  Examining the production of $\bar{d}$ at lower beam momenta (below 1.8 GeV/c) could open new avenues in $\bar{d}$ atomic physics, potentially enabling fully stopped $\bar{d}$ setups. Additionally, measuring the $\bar{d}$ yield across different momentum ranges may provide valuable insights into the $\bar{d}$ formation mechanism [20]. Because of the expected low yield at lower beam momentum, we will need longer beam time to accumulate enough statistics. We will start with the optimized setup at 1.8 GeV/c and gradually reduce the beam momentum to explore the $\bar{d}$ yield at lower momenta. We expect to complete this study with 16 hours of beam time.

4 Beam time request

To achieve the goals outlined in this proposal, we request a total of 24 hours of beam time at the J-PARC K1.8 beam line. This time will be divided into two parts: 8 hours for optimizing the $\bar{d}$ yield at 1.8 GeV/c and 16 hours for exploring the $\bar{d}$ yield at lower momenta.

Our proposed experiment is expected to be ready at any time during the J-PARC operation schedule. We aim to complete the proposed experiment by the summer of 2025 with the highest priority given to the optimization of $\bar{d}$ beam intensity at 1.8 GeV/c momentum (8 hours). In case additional beam time is available, we will also explore the $\bar{d}$ yield at lower momenta (16 hours).

5 Summary

We propose to investigate the antideuteron physics at J-PARC K1.8 beam line as a first step towards study antimatter composed of multiple antinucleons. The main topics to be addressed are the $\bar{d}-$nucleus optical potential and the multiple $\bar{N} - N$ annihilation mechanism.

To realize this program, we need to optimize first the $\bar{d}$ beam yield at the K1.8 beam line. The current $\bar{d}$ beam yield is ~ 0.3 $\bar{d}$/spill at 70 Tppp beam power. By tuning the beam line parameters, we expect to increase the $\bar{d}$ beam yield to much higher than ~ 1.0 $\bar{d}$/spill. We will also explore the $\bar{d}$ yield at lower momenta to investigate the $\bar{d}$ production mechanism and the high energy hadronization process.

References

[1] M. Ukai, *et al.*, arXiv:2312.11821

[2] Y. Ma, *et al.*, Letter of Intent: Investigating $\bar{d} + 12$C nucleus interaction at J-PARC, (2024)

[3] E. Widmann *et al.*, Hyperfine Interact. 240 (2019) 5

[4] The STAR Collaboration, Nature Physics 16 (2020) 409

[5] Angles & Demons (2009) directed by R. Howard, Columbia Pictures

[6] Th. Walcher *et al.*, Ann. Rev. Nucl. Part. Sci. 38 (1988) 67

[7] F. Binon *et al.*, Phys. Lett. B 31 (1970) 230

[8] S. P. Denisov *et al.*, Nucl. Phys. B 31 (1971) 253

[9] S. Acharya *et al.*, Phys. Rev. Lett. 125 (2020) 162001

[10] O. Chamberlain *et al.* Phys. Rev. Lett. 100 (1955) 947

[11] A. B. Larionov *et al.*, Phys. Rev. C 80 (2009) 021601

[12] E. Friedman *et al.*, Nucl. Phys. A 761 (2005) 283

[13] C. J. Batty, Rep. Prog. Phys. 52 (1989) 1165

[14] D. Garreta, *et al.*, Phys. Lett. 149B (1984) 64

[15] O. Buss *et al.*, Phys. Rep. 512, (2012) 1

[16] R. Subedi, *et al.*, Science 320 (2008) 1476

[17] Y. M. Antipov, *et al.*, Phys. Lett. 34B (1971) 164

[18] K. Yorita *et al.*, Proposal for Measurement of Anti-Matter Reaction in Liquid Argon Time Projection Chamber (LArTPC)

[19] J. R. Sanford and C. L Wang, BNL report 11479 (1967)

[20] F. Iazzi, Nucl. Phys. A 655 (1999) 371c